Mongolian Journal of Paleontology

Cite this article: Badamkhatan, Zorigt. and Idersaikhan Damdinsuren. 2021. A preliminary report on intraskeletal histological variation of basal neoceratopsian Protoceratops andrewsi. Mongolian Journal of Paleontology: 4, 38-44

Received: 10 December 2020
Accepted: 30 January 2021

Subject Category:
Geology and paleontology

Subject Areas:
paleontology

Keywords:
Dinosaur, ceratopsian, histology, microstructure, skeletochronology

Author for correspondence:
Zorigt Badamkhatan
e-mail: badmaa@mas.ac.mn

INSTITUTE OF PALEONTOLOGY
Mongolian Academy of Sciences

A preliminary report on intraskeletal histological variation of basal neoceratopsian *Protoceratops andrewsi*

Badamkhatan Zorigt[1], Idersaikhan Damdinsuren[1]

[1] Department of Paleozoology, Institute of Paleontology, Mongolian Academy of Sciences, Ulaanbaatar-15160, Mongolia

Determining relative age and growth stage of dinosaurs are crucial to understand dinosaur paleobiology. Various workers have determined growth rates of several dinosaur species based on multi skeletal elements. For age assessment, the most of current histological works rely on analyzing hind limbs such as femur and tibia. In this research, we compared microstructures of fore- and hind limb elements of ceratopsian dinosaur P*rotoceratops andrewsi.* Preliminary result shows that tibia and humerus may be viable candidates for determining relative age of *P. andrewsi.* However, histology of juvenile *P. andrewsi* exhibit slightly different histology.

INTRODUCTION

Bone histology has been playing an important role in the studies of dinosaur paleobiology. Many researchers have attempted to calculate relative age of dinosaur species using multi skeletal elements (Varricchio, 1993; Curry, 1999; Erickson and Tumanova, 2000; Horner and Padian, 2004; Reizner and Horner, 2006; Makovicky et al., 2007; Erickson et al., 2009; Horner et al., 2009; Erickson and Druckenmiller, 2011; Werning, 2012; Lee and O'Connor, 2013; Woodward et al., 2015). In order determine relative age, the hind limb elements such as femur, tibia, and fibula are preferred for histological analysis as they are believed to have the highest potential to preserve most of the lines of arrest-

ed growth (LAG) because of their low degree of remodeling (Horner et al., 1997). However, this appears to be applicable to facultative bipedal dinosaur species (Horner et al., 2000; Horner and Padian, 2004; Makovicky et al., 2006; Werning, 2012; Woodward et al., 2015; Badamkhatan, 2016; Idersaikhan et al., 2018). Fostowicz-Frelik and Słowiak (2018) have published a multi skeletal element study on *Protoceratops andrewsi.* The authors concluded that *P. andrewsi* limb elements show similar bone tissues. In this research, we hypothesize that fore- and hindlimb elements of quadrupedal dinosaur species such as *P. andrewsis* could exhibit same number of LAGs for age determination and growth development.

METHOD

We examined humeri, tibiae, and femora from three individuals of *P. andrewsi* (Ornithischia: Ceratopsia, Upper Cretaceous Djadokhta Formation, Mongolia). Based on the bone length, we classified the individuals in three different ontogenetic stages (Table 1). Bone microstructures were described using classification of Francillon-Vieillot et al. (1990). All specimens were sectioned at mid-shaft of the element. Diaphyseal region was removed from each femur, tibia, and humerus and molded for casting. Total of eighteen thin sections were prepared according to the methodology outlined in Lamm (2013).

Prepared thin sections were examined and photographed using a Nikon E600POL polarized petrographic microscope with AmScope MU500 camera. We used ImageJ Fiji v.1.53c (Schindelin et al., 2012) for quantitative measuring.

HISTOLOGIC DESCRIPTION

Stage 1 – 150814US-PJ-1

Humerus- The humerus cortex shows largely longitudinal vascularization. In the periosteal region, a small number of reticular vascularization is observed. Number of blood vessels is significantly reduced. The humerus shows fibro-lamellar bone with longitudinal vascularization. The density of osteocyte is high in the cortex. Two LAGs are preserved in the cortex.

№	*Specimen*	*Element length, mm*	*Estimated body length, cm*
1	Growth stage 1-(150814US-PJ-1) Humerus Femur Tibia	79	67
2	Growth stage 2-(MPC-ID 20090926) Humerus Femur Tibia	 192 204 225	133
3	Growth stage 3-(MPC-D100/530) Humerus Femur Tibia	 215 268 271	151

Table 1. Specimen numbers, sizes, and estimated body size. Body size was proportionally calculated by comparing femur length and body size of multiple complete specimens.

Femur- The femur cortex shows a combination of reticular and longitudinal vascularization with parallel-fibered bone matrix. In the lateral side of the cortex, reticular vascularization is the most prominent. The tibia cortex is consisted of plexiform bone tissue. The bone matrix contains high number of osteocyte lacunae. The specimen exhibits fibro-lamellar bone tissue. However, bone cortex exhibits five zones, the zones become

vague in anterior and lateral sides of the cortex. Total of four LAGs are observed in the cortex.

Tibia- The transverse sectional area of the tibia of the specimen is comprised mostly of longitudinal vascularization. The density of osteocyte lacunae is distributed evenly. The few number of secondary osteons are observed. The tibia consists of fibro-lamellar bone with longitudinal vascularization. There are only two observable zones in the cortex. Bone matrix is composed of parallel-fibered bone tissue. Three LAGs are preserved in the cortex (Fig. 1).

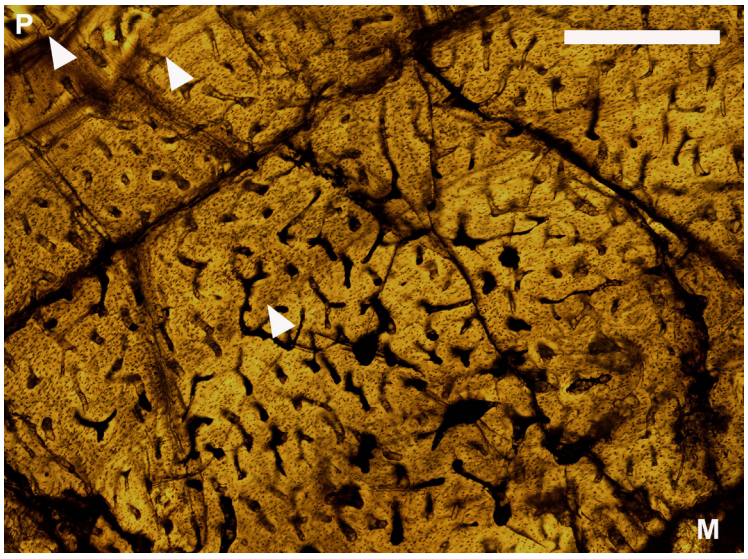

Figure 1. Transverse section of tibia representing growth stage 1. Bone tissue is consisted of mainly longitudinal and reticular vascularization with parallel-fibered bone matrix. P-periosteal region, M-medullary region, white arrows indicate lines of arrested growth. Scale bar equals 1 mm.

Stage 2 – MPC-ID 20090926

Humerus- The humerus presents plexiform and laminar bone tissues with primary osteons in circular rows (Fig. 2-A, B). Total of three zones are observed in the cortex. Osteoclastic activities are observed in the inner half of the cortex. The cortex contains three LAGs.

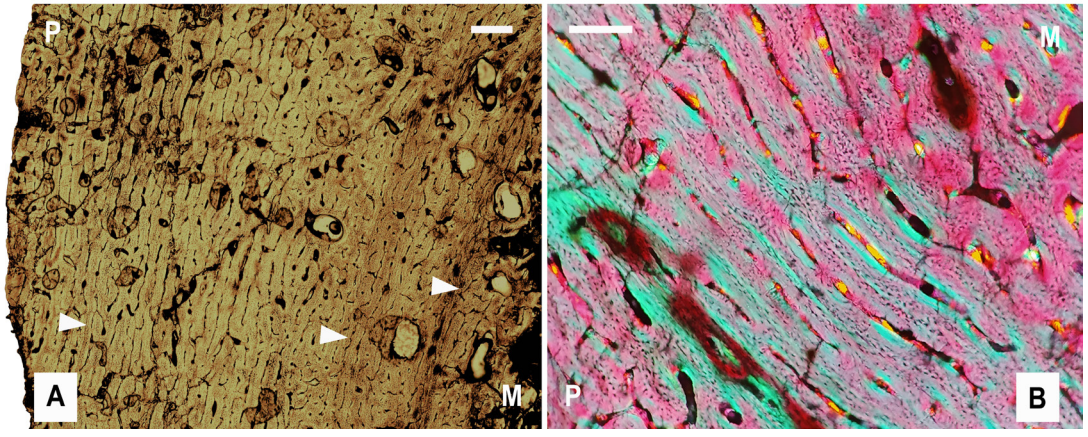

Figure 2. Transverse section of humerus representing growth stage 2. A) Humerus cortex is consisted of plexiform and laminar bone tissue. Bone tissue is consisted of mainly longitudinal and reticular vascularization with parallel-fibered bone matrix. Scale bar equals 1 mm. B) Laminar bone tissue with fibro-lamellar matrix. Scale bar equals 200 µm. P-periosteal region, M-medullary region, white arrows indicate lines of arrested growth.

Femur- The femur cortex contains a combination of longitudinal and reticular vascularizations. Three zones are observed. High number of osteocyte lacunae are preserved and distributed evenly. The femur presents reticular and plexiform bone tissues. In some small area of the outer cortex, the number of lacunae is reduced. Two LAGs are observed in the cortex.

Tibia- The tibia cortex exhibits longitudinal, reticular, and radial, and circular vascularizations. Four zones are observed in the cortex. The specimen is consisted of reticular and plexiform bone tissues. Circular vascularization is developing in outer half of the cortex. Beginning of laminar bone tissue is observed in the outer half of the cortex. Osteocyte lacunae are distributed evenly. Four LAGs are observed.

Stage 3 – MPC-D100/530

Humerus- The humerus cortex primarily exhibits a laminar bone tissue with longitudinal osteons. The cortex consists of parallel-fibered bone matrix. The number of osteons is reduced in the outer half of the cortex. Four LAGs are preserved in the cortex.

Femur- The femur shows laminar bone tissue with primary longitudinal vascularization. Four zones are observed in the cortex. This specimen does not contain no secondary osteons nor osteoclastic activity. Total of three LAGs in the cortex.

Tibia- The cortex is composed of laminar bone with primary osteons in circular row. Some small number of radial vascularization are developed in outer half of the cortex (Fig. 3). Osteoclastic activity is observed in the area near medullary cavity along with immature secondary osteons. Four LAGs are preserved in the cortex.

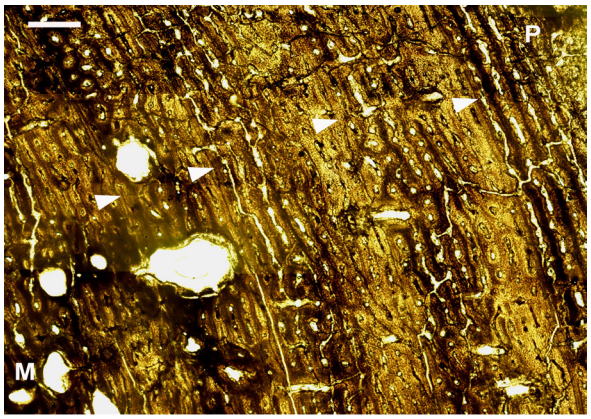

Figure 3. Transverse section of tibia representing growth stage 3. Bone cortex is organized in laminar bone tissue. Osteoclastic activities are observed inner cortex. P-periosteal region, M-medullary region, white arrows indicate lines of arrested growth. Scale bar equals 1 mm.

DISCUSSION

Skeletal elements of Stage 1

P. andrewsi present slightly different histological characters. The vascularity of long bones resembles reticular and longitudinal vascular canals. All elements contain fibro-lamellar bone tissue. Based on the vascularity, this individual was died while in actively growing age. However, LAG numbers vary in each bone. As Fostowicz-Frelik and Słowiak (2018) reported, limb elements show poor zonation. However, humerus of small individual exhibit multiple zones and LAGs in the cortex. The preserved LAGs variation in long bones of the juvenile is possibly caused of active bone remodeling during the fast growth age. In Stage 2, humerus, tibia, and femur present somewhat comparable histology. It was reported that humerus and tibia of subadult *P. andrewsi* exhibit similar histology, except femur which consisted of mostly woven-fibered bone tissue (Fostowicz-Frelik and Słowiak, 2018). The skeletal elements exhibit a formation of plexiform bone tissue with longitudinal and reticular vascularization. Inner half of humerus cortex contains active bone resorption. LAG numbers range between two

and four. MPC-ID 20090926 represents significant physiological change reflecting bone tissue transformation from reticular to plexiform bone tissue. It could possibly be caused by sexual maturity.

Laminar bone tissues are observed in Stage 3 individual. Large areas of the cortices were unable to observe due to poor preservation. The cortices are consisted of laminar bone tissue with parallel-fibered matrix. Tibia cortex shows a sign of osteoclastic activity in small area and immature secondary osteon.

CONCLUSION

Based on this study of histology of *P.andrewsi*, following conclusions are inferred:

1. Histologically, the most comparable limb elements of *P.andrewsi* include tibia and humerus. This result partially previous study on *P. andrewsi* histology (Fostowicz-Frelik and Słowiak, 2018).

2. Limb bone histology of *P.andrewsi* indicates a significant physiological change when body reaches approximately 133 cm in length.

3.The major weight bearing elements including tibia and humerus have a higher potential to preserve a greater number of the LAGs. These skeletal elements may provide sufficient information to reconstruct the relative age of *P. andrewsi* individuals at the time of death.

ACKNOWLEDGEMENTS

We would like to express our gratitude to Dr. Kh. Tsogtbaatar for encouraging us to conduct this study. We thank Mr. S. Baasankhuu and Ch.Bayardorj for technical support. We also grateful to team members of Mongolian-Japanese Joint Expedition for allowing us to utilize histological slides and specimens.

REFERENCES

Badamkhatan, Z., 2016. Histovariability and growth in the basal ceratopsian dinosaur *Psittacosaurus mongoliensis* from the Lower Cretaceous Khulsangol Formation, central Mongolia. Montana State University pp.

Curry, K. A., 1999. Ontogenetic histology of Apatosaurus (Dinosauria: Sauropoda): New insights on growth rates and longevity. Journal of Vertebrate Paleontology 19:654–665.

Erickson, G. M., and T. A. Tumanova. 2000. Growth curve of *Psittacosaurus mongoliensis* Osborn (Ceratopsia : Psittacosauridae) inferred from long bone histology. Zoological Journal of the Linnean Society 130:551–566.

Erickson, G. M., and P. S. Druckenmiller. 2011. Longevity and growth rate estimates for a polar dinosaur: a *Pachyrhinosaurus* (Dinosauria: Neoceratopsia) specimen from the North Slope of Alaska showing a complete developmental record. Historical Biology 23:327–334.

Erickson, G. M., P. J. Makovicky, B. D. Inouye, C. F. Zhou, and K. Q. Gao. 2009. A Life Table for *Psittacosaurus lujiatunensis*: Initial Insights Into Ornithischian Dinosaur Population Biology (vol 292, pg 1514, 2009). Anatomical Record-Advances in Integrative Anatomy and Evolutionary Biology 292:1684.

Fostowicz-Frelik, Ł., and J. Słowiak. 2018. Bone histology of *Protoceratops andrewsi* from the Late Cretaceous of Mongolia and its biological implications. Acta Palaeontologica Polonica.

Francillon-Vieillot, H., V. De Buffrénil, J. Castanet, J. Géraudie, F. J. Meunier, J. Y. Sire, L. Zylberberg, and A. De Ricqlès. 1990. Microstructure and mineralization of vertebrate skeletal tissues; pp. 471–548 in J. G. Carter (ed.), Skeletal biomineralization: patterns, processes and evolutionary trends. vol. 1. Van Nostrand Reinhold, New York.

Horner, J. R., and K. Padian. 2004. Age and Growth Dynamics of *Tyrannosaurus.* Proceedings: Biological Sciences 271:1875–1880.

Horner, J. R., K. Padian, and A. de Ricqlès. 1997. Histological analysis of a dinosaur skeleton: evidence of skeletal growth variation. Journal of Morphology 232:267.

Horner, J. R., A. De Ricqlès, and K. Padian. 2000. Long bone histology of the hadrosaurid dinosaur *Maiasaura peeblesorum* : growth dynamics and physiology based on an ontogenetic series of skeletal elements. Journal of Vertebrate Paleontology 20:115–129.

Horner, J. R., A. De Ricqles, K. Padian, and R. D. Scheetz. 2009. Comparative Long Bone Histology and Growth of the “Hypsilophodontid” Dino-

saurs *Orodromeus Makelai, Dryosaurus Altus,* and *Tenontosaurus Tillettii* (Ornithischia: Euornithopoda). Journal of Vertebrate Paleontology 29:734–747.

Idersaikhan, D., Z. Badamkhatan, and T. Chinzorig. 2018. Comparative long bone histology of ornithischian dinosaurs. Journal of Vertebrate Paleontology, Program and Abstracts, 2018 112.

Lamm, E.-T. 2013. Preparation and sectioning of specimens. Bone Histology of Fossil Tetrapods: Advancing Methods, Analysis, and Interpretation 55–160.

Lee, A. H., and P. M. O'Connor. 2013. Bone histology confirms determinate growth and small body size in the noasaurid theropod *Masiakasaurus knopfleri*. Journal of Vertebrate Paleontology 33:865–876.

Makovicky, P., K. Q. Gao, C. F. Zhou, and G. M. Erickson. 2006. Ontogenetic changes in *Psittacosaurus*: implications for taxonomy and phylogeny. Journal of Vertebrate Paleontology 26:94A.

Makovicky, P., R. Sadleir, P. Dodson, G. E. Erickson, and M. Norell. 2007. Life history of *Protoceratops andrewsi* from Bayn Zag, Mongolia. 67th Annual Meeting, Society of Vertebrate Paleontology. Program and Abstracts.

Reizner, J., and J. R. Horner. 2006. An ontogenetic series of the ceratopsid dinosaur *Einiosaurus procurvicornis* as determined by long bone histology. 66th Annual Meeting, Society of Vertebrate Paleontology. Program and Abstracts.

Schindelin, J., I. Arganda-Carreras, E. Frise, V. Kaynig, M. Longair, T. Pietzsch, S. Preibisch, C. Rueden, S. Saalfeld, B. Schmid, J.-Y. Tinevez, D. J. White, V. Hartenstein, K. Eliceiri, P. Tomancak, and A. Cardona. 2012. Fiji: an open-source platform for biological-image analysis. Nature Methods 9:676–682.

Varricchio, D. J. 1993. Bone microstructure of the Upper Cretaceous theropod dinosaur **Troodon formosus.** Journal of Vertebrate Paleontology 13:99–104.

Werning, S. 2012. The ontogenetic osteohistology of *Tenontosaurus tilletti*. PloS One 7:e33539.

Woodward, H. N., E. A. F. Fowler, J. O. Farlow, and J. R. Horner. 2015. *Maiasaura*, a model organism for extinct vertebrate population biology: a large sample statistical assessment of growth dynamics and survivorship. Paleobiology 41:503–527.